Expression and localization of a *Rhizobium*-derived cambialistic superoxide dismutase in pea (*Pisum sativum*) nodules subjected to oxidative stress

Aaron C. Asensio[1,§], Daniel Marino[2,5,§], Euan K. James[3], Idoia Ariz[1], César Arrese-Igor[2], Pedro M. Aparicio-Tejo[1], Raúl J. Arredondo-Peter[4], Jose F. Moran[1,*].

[1]*Institute of Agro-Biotechnology, IdAB-CSIC-UPNa-GN, Public University of Navarre, Spain*
[2]*Department of Environmental Sciences, Public University of Navarre, Spain,*
[3]*Scottish Crop Research Institute, Invergowrie, Dundee DD2 5DA, UK*
[4]*Laboratorio de Biofísica y Biología Molecular, Facultad de Ciencias, Universidad Autónoma del Estado de Morelos, Cuernavaca, Morelos, México*
[5]*Present address: Laboratoire des Interactions Plantes-Microorganismes, UMR CNRS 2594 – INRA 441, Chemin de Borde Rouge BP 52627, F-31326, Castanet-Tolosan Cedex, France*

[*]Corresponding author: **Jose F. Moran**
Institute of Agro-Biotechnology
IdAB-CSIC-UPNa-Government of Navarre
Public University of Navarre, Spain
E-31006 Pamplona, Navarra
Spain
Phone: +34 948168018
Fax: +34 948 168930
Email: jose.moran@unavarra.es

[§]Both authors contributed equally to this work

Abstract

Two phylogenetically unrelated superoxide dismutase (SOD) families i.e. CuZnSODs and Fe/Mn/cambialistic SODs, eliminate superoxide radicals in different locations within the plant cell. CuZnSODs are located within the cytosol and plastids, whilst the second family of SODs, which are considered to be of bacterial origin, are usually located within organelles, such as mitochondria. We have used the ROS-producer methylviologen (MV) to study SOD isozymes in the indeterminate nodules on pea (*Pisum sativum*). MV caused severe effects on nodule physiology and structure, and also resulted in an increase in SOD activity. Purification and N-terminal analysis identified cambialistic SOD (CamSOD) from the *Rhizobium leguminosarum* endosymbiont as one of the most active SODs in response to the oxidative stress. Fractionation of cell extracts and immunogold labeling confirmed that the CamSOD was present in both the bacteroids and the cytosol (including the nuclei, plastids and mitochondria) of the N-fixing cells, and also within the uninfected cortical and interstitial cells.

These findings, together with previous reports of the occurrence of FeSOD in determinate nodules indicate that Fe/Mn/Cam SODs have specific functions in legumes, some of which may be related to signaling between plant and bacterial symbionts, but the occurrence of particular isozyme(s) depends upon the nodule type.

Additional keywords: **Leghemoglobin, Superoxide dismutase, Paraquat, *Pisum sativum*, *Rhizobium leguminosarum*, Methylviologen, Reactive Oxygen Species**

Abbreviations: **ANA**, apparent nitrogenase activity; **ASC**, ascorbate; **CamSOD**, cambialistic SOD; **GSH**, reduced glutathione; **GSSG**, oxidized glutahione; **Lb**, leghemoglobin; **MV**, Methylviologen; **PVDF**, Polyvinylidene Fluoride; **PVPP**, polyvinylpolypyrrolidone; **ROS**, reactive oxygen species; **SOD**, superoxide dismutase**.**

INTRODUCTION

Reactive oxygen species (ROS) are unavoidable by-products of aerobic life, being constantly produced during normal metabolic processes, such as respiration, photosynthesis or biological N fixation. ROS production can also be crucial for plant growth, and its signaling role during plant-microbe interactions has been recently demonstrated during both pathogenesis and symbiosis (Marino *et al,* 2009; Torres 2010). However, when produced at high-levels as under biotic or abiotic stress, natural or induced senescence, or after exposure to xenobiotics, they can be lethal to cell integrity owing to their capacity to damage proteins, lipids and DNA (Apel and Hirt 2004).

Superoxide dismutases (SODs) act as a first line of defense against the superoxide radical (O_2^-). Two phylogenetically unrelated superoxide dismutase families, i.e. CuZnSODs and the group of Fe/Mn/cambialistic SODs, can be found in different locations within legume cells and rhizobial bacteroids (Bannister *et al*. 1987). Cytosolic and plastidial CuZnSOD isozymes are common to all plant cells, and are found in determinate and indeterminate nodules (Moran *et al*. 2003; Rubio *et al*. 2004; 2009). As well as being present in the cytoplasm of cells from various nodule types (Rubio *et al*. 2004; 2009), cytosolic CuZnSODs are also localized on chromatin in the nuclei of infected and uninfected cells in root nodules, stem nodules and leaves of the semi-aquatic tropical legume *Sesbania rostrata* (Rubio *et al*. 2009). Plastidial CuZnSOD isoenzymes are less abundant in nodules, as they are strongly linked to photosynthesis, but an exception are the photosynthetic stem nodules on *S. rostrata* (Rubio *et al*. 2009).

The second SOD family includes MnSODs, FeSODs and cambialistic SODs, which all share high protein sequence and structure similarity (Bannister *et al*. 1987; Alscher *et al*. 2002). MnSODs are typical bacterial and mitochondrial SODs, and in nodules are localized on bacteroids and on mitochondria within both infected and uninfected cells (Rubio *et al.* 2004, 2009). FeSODs have long been known to be associated with chloroplasts (Bannister *et al*. 1987; Alscher *et al*. 2002; Rubio *et al*. 2009), and, they are also found in phototrophic diazotrophic organisms, such as *Anabaena*, which exhibits a FeSOD specifically within heterocysts (Li *et al*. 2002). In legume nodules, in addition to an FeSOD being localized within plastids (Rubio et al. 2009), determinate nodule-forming legumes, such as cowpea and soybean, also have a distinct FeSOD in the cytosol, whose function has been suggested to be associated with nodule effectiveness (Moran *et al*. 2003). However, as yet, no FeSOD has been detected in the cytosol of classically indeterminate nodules, such as those on temperate crop legumes like pea (Moran *et al*. 2003), although it has been recently found to be associated with nuclear chromatin in nodules on *S. rostrata* (Rubio *et al*. 2009). Indeed, the role of non-plastidial Fe-containing SODs (and their essentiality) in various nodule types is not yet fully understood, especially as there is the intriguing possibility that in some nodule types (e.g. temperate indeterminate ones) the roles of FeSODs can be wholly or partially undertaken by a related group of bacterially-derived SODs, the so-called cambialistic SODs or CamSODs.

CamSODs, which have so far only been found in bacteria and diatoms, may have either Fe or Mn as a ligand, depending to the availability of these metals, and show differences in activity, pH and thermal stability depending on

the Mn/Fe content of the active centre (Santos *et al*. 1999; Ken *et al*. 2005). A cambialistic SOD has been shown to be required for effective nodule function in the *Medicago sativa – Sinorhizobium meliloti* symbiosis, but its role was considered exclusively to operate within the bacteroids (Santos *et al*, 1999; Santos 2000), and little else is known about it in terms of its activity or location within nodules. In this study we have applied methylviologen (MV), a compound sometimes referred to by the commercial name Paraquat, which exacerbates O_2^- production in the nutrient solution of nodulated pea plants to provoke a mild oxidative stress, and thereby induce the antioxidant systems that allowed for the better study of the SOD protein family in pea nodules. We report the induction of elevated bacterial cambialistic SOD activity which was found to be localized not only within the *Rhizobium* microsymbiont but also within different plant cell compartments of both infected and uninfected cells.

RESULTS

Effect of Methylviologen-mediated oxidative stress on nitrogen fixation and nodule functioning

We applied MV in the nutrient solution of plants growing in hydroponic culture. This resulted in a more homogeneous application compared to using a short spot foliar application, and thus imposed a more progressive oxidative stress on the nodules whilst avoiding a strong effect on the shoot that would have caused rapid plant death. As well as affecting plant growth and photosynthesis, the MV treatment also markedly decreased nitrogen fixation almost to the point of cessation (Table 1). Nodule plant-fraction protein contents

were also significantly reduced (-35 %) by MV stress, but bacteroid protein contents were relatively unaffected (-11%). Among the proteins and enzymes analysed the most striking effect of MV was on Lb, the main cytosolic protein within the nodule (ca. 1 mM), which suffered an 82% reduction in concentration (Table 1). The MV treatment also evidently caused an alteration in the nodule cell redox state, as ASC and GSH, which are the main soluble antioxidants within nodules, were highly oxidized resulting in a striking 75% decline in both ASC/DHA and GSH/GSSG ratios (Table 1).

The MV application adversely affected nodule structure, as can be seen by light microscopy (LM) and transmission electron microscopy (TEM) (Fig. 1). Nodules from untreated control plants had infected cells that were typically turgid with a round central vacuole (Fig. 1A). These were packed with bacteroids surrounded by a symbiosome membrane, so that there was a very narrow space between bacteroids and the symbiosome membrane (Fig. 1B). Both the bacteroid and host cell cytoplasm was electron dense, with the host cytoplasm containing numerous intact organelles (Fig. 1B). However, at a relatively low concentration of MV (1 μM) degradation of infected cells was evident, with the formation of large vacuoles (Fig. 1C), and at the ultrastructural level it could be seen that these were formed largely through the expansion of the symbiosome spaces, so that they coalesced into larger vacuoles (Fig. 1D). The bacteroids were distorted in shape compared to controls and were less electron dense, suggesting that they were losing cytoplasmic integrity (Fig. 1D). At a higher concentration of MV (10 μM) both infected and uninfected cells appeared to be plasmolysed ie. they were distorted in shape and without a central vacuole, with the cell contents pulled away from the cell wall (Fig. 1E).

The bacteroids, which were now very distorted in shape, were no longer surrounded by intact symbiosomes, and the host cytoplasm had been reduced to fragments (Fig. 1F). Interestingly, the bacteroids in nodules subjected to both MV treatments could still be immunogold labeled with an antibody against the nifH protein (Fe-protein) of the nitrogenase enzyme complex (Fig. S1).

Effect of Methylviologen-mediated oxidative stress, ageing and excess Fe* on *SOD isozymes in pea nodules

Nodules and leaves from pea plants showed different patterns of SOD activity (Fig. 2). Four isozymes were found in nodule tissues, whilst 5 different bands could be observed in leaves (Fig. 2A). Based on their mobility in native gels and their differential inhibition by KCN (Fig. 2B) or H_2O_2 (Fig. 2C), a MnSOD and cytosolic/plastidial CuZnSODs could be easily identified (Fig. 2 B,C). A fourth band, with a mobility intermediate between MnSOD and cytosolic CuZnSOD showed strong activity (Fig 2A); this SOD exhibited a mobility typical of an FeSOD isozyme, but it resisted the cyanide (Fig 2B) and hydrogen peroxide (Fig 2C) treatments which characterize MnSODs and CamSODs (Santos *et al*. 1999). Although this putative CamSOD was not present within the leaf extracts, two FeSODs could be observed that were not present in nodules (Fig. 2A).

The SOD activities of nodules were affected by the MV-mediated oxidative stress, with the putative CamSOD showing one of the greatest increases (+84%) amongst the responses of all the SOD isozymes to MV application (Fig. 2A). The gels in Fig. 2 are representative examples of four replicate experiments. In each experiment the total activity of the CamSOD was the highest amongst all the SOD isozymes examined. Large increases after MV

treatment were also observed in the nodule activities of cytosolic CuZnSOD (+157%) and (to a lesser extent) of MnSOD (Fig. 2A). In contrast, the plastidic CuZnSOD activity, although it increased after application of MV, still represented a low proportion of the total SOD activity in nodules (Fig. 2A). In leaves, the activity of the cytCuZnSOD isozyme was significantly induced after application of MV, whilst those of plCuZnSOD and FeSOD were virtually unchanged (Fig. 2A).

In order to study the effects of age on the SOD activities of pea nodules, analyses were performed on nodule populations from plants up to 10 weeks old (Fig. 3). Although the putative CamSOD again showed the highest activity, no important differences in activity of any SOD isozymes were found associated with increasing nodule age. The exception was in extracts of nodules from plants at 10 weeks which showed a slight decrease in intensity of the putative CamSOD band and an increase in intensities of the two CuZnSOD bands compared to extracts from younger nodules (Fig. 3). The response of nodule SODs to Fe excess was also determined in an attempt to elucidate the regulating role of Fe in CamSOD activity; a treatment with Fe(III)-EDTA increased the activity of the putative CamSOD activity, whilst the plant mitochondrial MnSOD was increased at a lower extent (Fig. 4). On the contrary, both CuZnSODs isozymes were reduced in activity.

Identification of a cambialistic SOD from* Rhizobium leguminosarum *within pea nodule extracts

The putative CamSOD was purified after anion exchange chromatography using a MonoQ column, native gel PAGE and SDS-PAGE.

After transfer to PVDF membranes and staining, a major band was visualized between 22 and 28 kDa (Fig. 5). This band was further examined by N-terminal sequencing, and the 18 initial residues found for the polypeptide were NH_2^+-AFELPELPYDYEALAPFM, which corresponded to the N-terminal sequence of the protein encoded by the *sodA* gene of *R. leguminosarum*, a cambialistic SOD (UniProtKB accesion number Q1MJM3-1; Young *et al*. 2006). The protein has 200 amino acids and a theoretical molecular mass of 22 kDa which matches the size of the band purified for sequencing (Fig. 5). The putative CamSOD from *R. leguminosarum* shares high similarity (86 %) to the *S. meliloti* cambialistic SOD protein and to a putative camSOD from *Brucella ceit* (83 %). This homology, together with the reported mobility of the protein and its tolerance to peroxide (Fig. 2), are strong evidence that this putative camSOD is, in fact, a true camSOD. Moreover, an analysis of the metals in one of the purified camSOD batches demonstrated the presence of Mn but not of Fe (not shown).

An antibody against the CamSOD was raised in rabbits for immunological assays. Based on the sequence of the protein (Fig. 6) and its 3D-protein model (Fig. S2), a peptide was selected in an exposed position of the 3D structure that would theoretically allow the use of the antibody under non-denaturing conditions. To test the specificity of the antibody, two different immunoblots were conducted (Fig. 7). The first, under denaturing conditions, showed only one band at the molecular weight expected for the CamSOD (Fig. 7A). The second immunoblot was from a native-PAGE gel with two sets of pea root and nodule extracts loaded onto it. One set of root/nodule extracts was subsequently excised from the gel and transferred to a PVDF membrane and used for an immunoblot, whilst the other was stained using an *in-gel* SOD activity assay; only one band was detected in nodule extracts under native

conditions, and this was at the same weight as the CamSOD activity detected by the in-gel SOD activity assay (Fig. 7B). CamSOD protein or activity was not detected in root extracts (Fig. 7B), thus indicating its specificity to nodular tissue.

Subcellular localization of CamSOD

We showed above that CamSOD is one of the main responsive SODs in activity assays of nodule extracts exposed to MV-mediated oxidative stress (Fig. 2). These extracts were presumed to be free of bacteroids because of the extraction method used to obtain them, but in order to confirm that CamSOD was present within the plant fraction of nodules even though it is encoded by the rhizobial microsymbiont, nodule compartments were fractionated using a very mild protein extraction followed by differential centrifugations. Immunoblots using the anti-CamSOD antibody and an anti-nitrogenase (anti-nifDK) antibody were performed (Fig. 8) on the fractions obtained, and the results indicated that the CamSOD enzyme was present in free-living bacteria, bacteroids, and also the plant soluble fraction (Fig. 8A). Interestingly, a band at approx. 50 kDa was observed in the crude extract and in the plant fraction samples, and this was more intense in the MV-treated samples. The immunoblot using the anti-nifDK antibody showed that although nitrogenase enzyme was present in bacteroids and crude extracts, the plant cell fraction was free of broken bacteroids, both in control and MV-treated nodules (Fig. 8B).

Immunogold labeling was used to ascertain the exact location of CamSOD within pea nodules (Fig. 9). In infected cells of untreated control nodules, in addition to bacteroids (Fig. 9A) and bacteria within infection threads

(Fig. 9B), which were labeled as expected, CamSOD localization was also observed within the host cytosol (Fig. 9A – C) and their nuclei (including chromatin) (Fig. 9C). Mitochondria were labeled in both infected and uninfected cells, as were plastids (Fig. 9D). Interestingly, CamSOD was localized within all symplastic subcellular compartments/organelles (except for the vacuole) in all cell types throughout the nodule. CamSOD could also be localized on bacteroids within MV-treated nodules, but localization was less evident in the plant cytosol and organelles (Fig. 9E), probably at least partly because the plant fraction was so degraded by the treatment (Fig. 1F). Sections of control nodules treated with the pre-immune serum showed no significant gold labeling (Fig. 9F). Also, labelling with anti-nifH antibody was used as control of the intactness of the bacteroids during the immunogold. Immunolocalization of nifH protein was restricted to bacteroids for all treatments (Fig. S1).

SodA gene upstream and downstream sequences analysis

Based on the *R. leguminosarum* chromosome sequence, putative promoters were studied within the surroundings of the *SodA* gene. The search for putative promoter boxes provided a number of potential sequences upstream of the *sod* gene, including those for canonical -10 and -35 boxes, oxygen- and ROS-response proteins, regulators of the Arg metabolism and control of quorum-sensing genes (Fig. S3). One of these is the OxyR transcription factor-regulated promoter, which is regulated by hydrogen peroxide produced via the activity of SODs. The OxyR-regulated promoter is known to trigger the cellular anti-oxidative response including the induction of SODs (Gonzalez-Flecha and Demple, 2000).

A search for coding sequences flanking the *sodA* gene in the *R. leguminosarum* genome revealed that genes coding for proteins functioning in drug resistance and detoxification, as well as redox-acting proteins exist in proximity to the *sodA* gene (Fig. S4).

DISCUSSION

Methylviologen application caused an oxidative stress in pea nodules

The application of 10 μM MV in the nutrient solution of nodulated pea plants provoked severe adverse effects on shoot and nodule physiology related to ROS production. The Lb reduction after MV treatment (Table 1) was particularly striking, as total nodule soluble proteins were much less affected by MV than Lb. Lb has been previously shown to be extremely sensitive to redox changes *in vitro* and *in vivo* (Marino *et al*. 2009) and, indeed, the degradation of Lb has been indicated as a useful marker of nodule oxidative stress (Dalton, 1995; Marino *et al*. 2006). Moreover, the onset of the oxidative stress in pea plants has been related in part to the release of Fe from the heme group of Lb, since Fe contributes to the conversion of H_2O_2 and superoxide radicals into extremely reactive hydroxyl radicals (Gogorcena *et al*. 1995). Also, Lb is the main reservoir of O_2 in the nodule cytosol, and its autoxidation generates the superoxide radical (Puppo *et al*. 1981). Indeed, a strong effect of a superoxide-generating molecule, such as MV, would be expected on nodule performance, as it uses oxygen molecules to transfer electrons, and hence generates superoxide radicals (Bus *et al*. 1976). Therefore, the observed decline in BNF under oxidative stress, which was almost a complete suppression of the

process, may be attributed more to a reduction in Lb content than to a direct effect on nitrogenase activity. This is also supported by the ultrastructural observations which showed that MV application resulted in severe degradation of the host cytosol, but left many of the bacteroids intact (albeit in distorted forms).

In general, the data in the present study indicate that MV has a stronger effect on nodules than on the aerial part of the plant. This is expected because MV is affecting primarily those organs that are directly in contact with the hydroponic solution that contains it (i.e. the roots and nodules), and this most likely explains why the proportional decrease in N_2 fixation was greater than that of photosynthesis.

Methylviologen application induced the expression of a novel cambialistic SOD in pea nodules

We show that MV caused alterations in the pattern of SOD isozyme activities of nodule extracts, and to a lesser extent within the leaf extracts (Fig. 2). The physiological, anatomical and protein/Lb-content data suggest that the nodule cytosol is a cell compartment strongly affected by ROS overproduction. The CamSOD, which exhibits a similar mobility to FeSODs, proved to be one of the main responsive SODs in pea nodules, although it was absent in leaves or roots (Figs. 2 and 7). A pea nodule SOD has previously been shown to be an important responsive enzyme to MV application (Marino *et al*. 2008), and this was considered to possibly be a FeSOD based on its mobility in native gels. However, the present study has categorically identified this SOD as a CamSOD by isolating the active enzyme followed by SDS-PAGE, and subsequent N-

terminal sequencing. Interestingly, a loss of the initial methionine residue of the CamSOD protein at the N-terminus was observed (Fig. 6). The cytosolic FeSOD from cowpea also loses 6 aminoacids from the N-terminus (Moran *et al*. 2003), and a similar initial loss of methionine was reported in FeSOD from *Anabaena* (Li *et al*. 2002); the authors of the latter study suggested that this loss of amino acids was most likely due to posttranslational removal.

High antibody specificity is crucial for the legitimacy of the immunogold labelling studies. The immunoblot experiments showed that the polyclonal antibody we raised in rabbits against a CamSOD epitope showed no cross-reaction with other related SODs, such as plastidial FeSODs or MnSOD of either bacterial or plant origin, even using the antibody at 1:1000 dilution, the same as was used in the immunolocalization experiments (Fig. 7). Also, it is remarkable that the anti-nif DK antibody which was used as a control to confirm that bacteroids remained intact during the mild SOD extraction (Fig. 8b) only detected nitrogenase in crude nodule and bacteroidal extracts, but not in the plant-fraction extracts. This fractionation of the pea nodule extract was our first indication that the CamSOD was present in the plant fraction, and that its presence was not due to the lysis of bacteroids. Interestingly, a 50 kDa band was apparent in MV-treated plant and nodule fractions (Fig 8a). This band, which may well correspond to an aggregation form resistant to the SDS-PAGE conditions, arose from oxidation of CamSOD due to the action of MV. An auto-oxidative mechanism has been proposed for the human cytosolic CuZnSOD1 resulting in an aggregation of the enzyme (Hart 2006), and studies using cell culture models have demonstrated that detergents or denaturing agents are unable to dissociate these aggregates (Perry *et al*. 2010).

Secretion of the CamSOD enzyme from bacteroids and its function in the plant fraction

The CamSOD appears not to be secreted by a classical secretory pathway, as it lacks a putative transit peptide, as indicated by the SignalP software and SecretomeP (Bendtsen *et al*. 2005). Several types of secretory pathways for proteins have been studied in *R. leguminosarum*, and many bacterial proteins have been found to be secreted without any apparent signal peptide, and yet they have been shown to actively participate in biological processes in the extracellular environment (Krehenbrink and Downie 2008). These include several bacterial SODs, such as *M. tuberculosis SodA* (Bendtsen *et al* 2005). Given that we have observed a bacterial protein (ie. CamSOD) within several subcellular locations in both infected and uninfected cells in pea nodules, and that non-classical secretion systems are present in bacteria, as well as in eukaryotic cells in plants, and are involved in the secretion of several proteins including SODs (Agrawal *et al* 2010), it is reasonable to postulate that this system is also used in legume nodules for the transport of bacterial CamSODs (and possibly other SODs; Rubio *et al*. 2009) from the cytoplasm to organelles and adjacent cells.

With regard to the extracellular secretion of SODs, the non-pathogenic mycobacterium *M. smegmatis* does not secrete SodA but, interestingly, in the pathogenic *M. tuberculosis* SodA is secreted in a SecA2 protein dependent manner. Indeed, SecA2 deletion abolishes SodA secretion in mice suggesting that non-classical secretion systems are required for SodA export (Bendtsen *et al* 2005). Furthermore, in *Xanthomonas campestris* pv. *campestris* (Xcc) one of

the most abundant proteins of the extracellular proteome is SodM, a CamSOD homologue, which also lacks a secretion signal (Watt *et al*. 2005). This protein has been described as an inducible elicitor of an oxidative burst in tobacco cell suspension cultures. Smit *et al*. (1996) showed the induction of SodM in *Xanthomonas* 3-4 h after its inoculation onto turnip and pepper plants, and they suggested that it may be a defensive reaction of the bacteria to the hypersensitive-response from the plant. The extracellular location of the Fe/Mn/CamSOD family of enzymes has been reported for several other bacteria, such as *Streptomyces* (Folcher *et al*. 2001; Langlois *et al*. 2003), cyanobacteria (Ehling-Schulz *et al*. 2002), and *Streptococcus* (McMillan *et al*. 2004). Taken together, these data suggest that CamSOD excretion in pea nodules may be part of the plant-bacterial crosstalk aimed at de-activating the hypersensitive response by the pea plant, and this role might also be extended to other FeSODs in legumes.

Santos *et al*. (1999; 2000) have demonstrated using *S. meliloti* mutants that the absence of the CamSOD triggers early senescence both in the nodules, as well as in the whole alfalfa plant, and thus confirmed its requirement for nodule effectiveness. In our study, we show that CamSOD is induced by oxidative stress concomitantly with the degradation of substantial amounts of Lb. Paradoxically, despite its high sensitivity to ROS, Lb is considered to be a very important source of superoxide radicals in the nodule cytosol (Dalton, 1995), and it has been shown that ROS production is attenuated when Lb is absent eg. in *Lotus japonicus* Lb-deficient mutants (Günther *et al*. 2007). Furthermore, Lb degradation is exacerbated under stress conditions and during senescence (Gogorcena *et al*. 1995; Table 1), both of which may well increase

the concentrations of free Fe in the pea nodule cytosol and hence lead to a substantial increase in free radical production (Gogorcena *et al*. 1995). Thus, it is likely that SODs will provide antioxidant protection in the nodule cytosol under such conditions. In cowpea, the cytosolic FeSOD is related to fully operational nodules since its expression increases in mature nodules, but it also increases during nodule senescence. As its expression is correlated with Lb synthesis and degradation, it was suggested that cowpea cytosolic FeSOD is regulated in some way by free Fe or heme availability (Moran *et al*. 2003). In addition, other antioxidant enzymes, such as catalase and ascorbate peroxidase, are up-regulated in plants exposed to excess Fe, and Fe-induced oxidative stress has been proposed as a trigger for ferritin up-regulation (Lobréaux *et al*. 1995). In the present study, we have observed that the CamSOD activity in pea nodules markedly increases when they are grown under conditions of excess Fe (Fig. 4). It has been shown that Fe^{2+} enters the bacteroid through a divalent metal transporter located in the peribacteridal membrane which is synthesized by the plant (Kaiser *et al*. 2003) and, therefore, CamSOD synthesis in the bacteroid may be regulated by both the plant and bacterial symbionts via the nodule Fe content.

CamSODs and their related proteins, cowpea nodule FeSOD and the FeSOD of *Sesbania rostrata* root and stem nodules, have all been localized within the cytosol (Moran *et al*. 2003; Rubio *et al*. 2009; this study). Taken together, these results indicate the widespread occurrence of Fe/Mn/CamSODs in the cytosol of legume nodules, and the fact that they are mostly absent from the cytosol of non-legumes suggests that they possibly represent a specialized antioxidant mechanism related to the symbiotic N fixation process in nodules.

Pea plants have previously been shown to have active FeSODs within plastids (Iturbe-Ormaetxe *et al*. 1998; Ariz *et al*. 2010; Rubio *et al*. 2009; this work), but a more novel location of FeSOD was recently shown for *S. rostrata* root and stem nodules where it was localized in the nuclei, particularly on the chromatin (Rubio *et al*. 2009). We have seen similar results in the present study of pea nodules for the CamSOD, thus suggesting a possible role for FeSODs/CamSODs in the protection of chromatin from ROS. However, as ROS are signaling molecules and all signaling systems need a terminator signal, we cannot discard the possibility that SODs in nuclei are performing this role as part of the signaling system. As the superoxide radical is a charged molecule with a very short life, and hence has restricted mobility through membranes, the question remains as what would be the mechanism and/or the conditions under which superoxide radicals are being transported into and/or produced within the nuclei.

In conclusion, in this work we have purified and identified a cambialistic SOD from *Rhizobium leguminosarum*, and furthermore have shown that it is one of the most responsive SOD isozymes against MV-generated oxidative stress in pea nodules. Biochemical assays and immunolocalization studies have demonstrated that CamSOD is present not only in bacteroids but also within the cytosol of both the infected N_2-fixing cells and the uninfected cortical and interstitial cells. These findings have thus suggested export of the CamSOD from the bacteria to the plant cells via non-classical secretion systems. Finally, these results indicate that Fe/Mn/Cam SOD isozymes may have specific functions in both indeterminate and determinate nodules, including signaling

between the plant and the bacterial symbionts, and /or elimination of superoxide in the nucleus.

MATERIALS AND METHODS

Plant material and treatments

Pea seeds (*Pisum sativum* L. cv. Sugar-snap) were grown as described in Marino *et al*. (2008). Single plants were inoculated with *Rhizobium leguminosarum* biovar. *viciae* strain NLV8 one week after sowing when seedlings had reached a height of 2-3 cm. Plants were grown in pots in a 1:1 (v:v) perlite:vermiculite mixture at 22/18ºC day/night temperature, 70% relative humidity, 500 µmol photons m^{-2} s^{-1}, 15 h photoperiod and were watered with a N-free nutrient solution. Four week-old plants were transferred to 1 L hydroponic tanks four days prior to treatment imposition.

For the MV treatments, plants were divided randomly into two sets, which were exposed to 0 (controls) or 10 µM methylviologen hydrate (Sigma-Aldrich, St. Louis, MO) for 96 h. Plant dry weights were determined after drying for 48 h at 80ºC. Fresh nodule aliquots were immediately frozen in liquid nitrogen and stored at –80ºC for analytical determinations. For the Fe-excess treatment, four week-old plants were divided randomly into two sets, which were exposed for 24 h either to 100 µM Fe(III)-EDTA or to 100 µM Na_2-EDTA (control). To determine the effects of increased nodule age on the response of nodules to MV plants were grown for 10 weeks.

SOD activity staining

The SOD isozyme pattern was analyzed by activity staining following electrophoresis on 15 % non-denaturing polyacrylamide gels. Nodules

or roots were ground with an extraction buffer consisting of 50 mm potassium phosphate (pH 7.8), 0.1 mm EDTA, 0.1% (v/v) Triton X-100, and 1% (w/v) polyvinylpyrrolidone-10. The extract was filtered through cheesecloth and centrifuged at 12,000*g* at 4°C for 20 min to remove cell debris. Samples were electrophoresed and gels were stained based on the inhibition of the reduction of nitro blue tetrazolium (NBT) by superoxide radicals generated photochemically (Beauchamp and Fridovich 1971). The identification of the different isozymes was based on the differential inhibition of SOD activity on gels preincubated with either 3 mM KCN or 5 mM H_2O_2 for 1 h.

Physiological and biochemical parameters.

The contents of ascorbate (ASC), dehydroascorbate (DHA), reduced and oxidized glutathione (GSH and GSSG respectively) in nodule extracts were analysed by high-performance capillary electrophoresis as described by Zabalza *et al*. (2008). Protein and leghemoglobin (Lb) determinations were performed as described in Marino *et al*. (2006).

SOD purification and N-terminal sequencing

Seventeen g of nodules were homogenized using a pestle and mortar with the addition of 50 mL of 100 mM potassium phosphate buffer (pH 7.8) containing 0.1 mM EDTA and 5 g PVPP. The resulting sample was filtered through a Miracloth sheet and centrifuged for 20 min at 18000 x *g*. The supernatant was dialyzed against column buffer (10 mM potassium phosphate buffer, pH 7.8) and loaded into a 5 ml Hitrap-DEAE Sepharose fast flow column (GE Health care, Piscataway, NJ), and a 100 mL gradient of potassium phosphate buffer (pH 7.8) ranging from 10 to 100 mM was used to release the

protein from the column. Fractions were assayed using the SOD activity assay, and those containing CamSOD were pooled, dialyzed and applied to a HiTrap-Mono Q Sepharose Fast flow column (GE Health-care, Piscataway, NJ) column equilibrated with the column buffer described above. Protein was eluted using a gradient of 0 to 500 mM NaCl in 10 mM potassium phosphate buffer (pH 7.8). Fractions were assayed *in gel* for SOD activity, and active camSOD bands from native gels were excised, eluted from the gels, concentrated and loaded onto SDS gels as described by Moran *et al*. (2003). The SDS gels were transferred to PVDF membranes, and N-terminal sequencing was performed on selected bands by Edman degradation.

Fractionation of nodule extracts

Fresh nodules were homogenized with a pestle and mortar in potassium phosphate buffer (50 mM pH 7.4) plus mannitol 0.2 M, and then filtered. This crude extract was immediately centrifuged for 5 min at 400 x *g*. The pellet, largely consisting of cell debris, was discarded, and the supernatant was centrifuged again for 10 min at 2500 x *g*. After this step, the supernatant mainly consisted of cytosolic and particulate cell components, whilst the pellet was mainly bacteroids (adapted from Trinchant *et al*. 2004).

Antibody production and protein inmunoblotting assays

For CamSOD antibody production the peptide KNGKLEISKTPNGE was selected on the basis of its antigenic properties and its exposed position in the protein structure (Fig S2). This peptide was chemically synthesized (Thermo

scientific, Beverly, MA), and used for rabbit immunization and IgG purification (Biogenes, Berlin, Germany).

Protein extracts (5 µg of protein per lane for anti-nifDK and 30 µg for anti-CamSOD) were loaded onto 12% (w/v) SDS-PAGE, and electroblotted onto 0.45 µM polyvinylidene difluoride membranes (Pall Corporation, Pensacola, FL). Either anti-camSOD or anti-nitrogenase (anti-nifDK; Allen *et al*. 1993) primary antibodies were used at 1:10.000 dilution, except for Fig. 7, where a dilution of 1:1000 of anti-camSOD was employed. The secondary antibodies employed in the assays were goat anti-rabbit IgG alkaline phosphatase conjugate (1:10,000, v/v; Sigma-Aldrich, St. Louis, MO) or horseradish peroxidase conjugate (1:20,000, v/v; Sigma-Aldrich, St. Louis, MO). Immunoreactive bands were visualized with the NBT/5-bromo-4-chloro-3-indolyl-phosphate system (Sigma-Aldrich, St. Louis, MO) or with a chemiluminescent substrate (SuperSignal West Pico, Pierce, Rockford, IL), respectively.

Microscopy and immunogold labeling

Fresh samples of control and MV-treated pea nodules were fixed and embedded for light microscopy and transmission electron microscopy (TEM) according to Madsen *et al*. (2010). Briefly, nodules were fixed in 2.5 % glutaraldehyde in 0.1 M sodium cacodylate (pH 7.0) overnight at 4 °C and subsequently dehydrated in an ethanol series, and embedded in LR White acrylic resin (Agar Scientific). Semithin sections (1 µm) were taken for light microscopy and ultrathin (80 nm) sections were taken for TEM using a Leica UCT ultramicrotome. The semithin sections were collected on glass slides and stained with 0.1 % toluidine blue, whereas the ultrathin sections were collected

on pioloform-coated nickel grids and immunogold labelled with an antibody against the nifH protein of *Rhodospirillum rubrum* (diluted 1:100) or with the CamSOD antibody (diluted 1:1000) according to the protocols of Rubio *et al*. (2009). The ultrathin sections were stained with uranyl acetate for 10 min before being viewed and digitally photographed using a JEM 1400 transmission electron microscope (JEOL). For negative controls, serial sections were immunogold labelled with pre-immune serum (diluted 1:1000).

In silico analysis

Swiss-Model software of the Swiss Institute of Bioinformatics was used for generate a 3-D model of the *Rhizobium leguminosarum* CamSOD protein (UniProtKB/TrEMBL accession number: Q1MJM3-1). The CamSOD sequence was analyzed with the Signal P, and SecretomeP 2.0 software (Center for Biological Sequence Analysis, Technical University of Denmark) in order to search for possible classical and non-classical protein secretion signals (Bendtsen *et al*. 2004; Bendtsen *et al*. 2005).

ACKNOWLEDGMENTS

Authors wish to thank Dr. Paul Ludden and Dr Agneta Noren, respectively, for the kind gifts of the anti-nitrogenase nif-DK and nifH antibodies, and to Dr. Esther M. González and Dr. Estíbaliz Larrainzar for help with table I and with the fractionation experiments, respectively. This work was supported by the Spanish MICIIN (grants no. AGL2007-64432/AGR and AGL2010-16167). ACA was supported by a doctoral contract within Euroinnova Navarra Programme (Expte. IIM10784.RI1), Government of Navarra, Department of Innovation,

Business and Employment. IA was supported by a doctoral Fellowship from the Public University of Navarre.

LITERATURE CITED

Alscher, R.G., Erturk, N., and Heath L.S. 2002. Role of superoxide dismutase (SODs) in controlling oxidative stress in plants. Journal of Experimental Botany 53:1331-1341.

Agrawal, G.K., Jwa, N.S., Lebrun, M.H., Job, D. and Rakwal, R. 2010. Plant secretome: Unlocking secrets of the secreted proteins. Proteomics.10:799-827.

Allen, R.M., Homer, M.J., Chatterjee, R., Ludden, P. W., Roberts, G.P. and Shah, V.K. 1993. Dinitrogenase reductase- and MgATP-dependent maturation of apodinitrogenase from *Azotobacter vinelandii*. Journal Journal of Biological Chemistry. 268:23670-23674.

Apel, K. and Hirt, H. 2004. Reactive oxygen species: Metabolism, oxidative stress, and signal transduction. Annual Review of Plant Biology 55:373-399.

Ariz, I., Esteban, R., García-Plazaola, J.I., Becerril, J.M., Aparicio-Tejo, P.M. and Moran, J.F. 2010. High irradiance induces photoprotective mechanisms and a positive effect on NH_4^+ stress in *Pisum sativum* L. Journal of Plant Physiology 167:1038-45.

Bannister, J.V., Bannister, W.H. and Rotilio, G. 1987. Aspects of the structure, function and applications of superoxide dismutase. CRC Critical Review in Biochemistry 22:111-180.

Beauchamp, C. and Fridovic, I. 1971. Superoxide dismutase - Improved assays and an assay applicable to acrylamide gels. Analytical Biochemistry 44:276-287.

Bendtsen, J.D., Nielsen, H., von Heijne, G. and Brunak, S. 2004. Improved prediction of signal peptides: SignalP 3.0. Journal of Molecular Biology 340:783-795.

Bendtsen, J.D., Kiemer, L., Fausboll, A. and Brunak, S. 2005. Non-classical protein secretion in bacteria. BMC Microbiology 5:58.

Bus, J.S., Aust, S.D. and Gibson, J.E. 1976. Paraquat toxicity - Proposed mechanism of action involving lipid peroxidation. Environmental Health Perspectives 16:139-146.

Dalton, D.A. 1995. Antioxidant defenses in plant and fungi. Pages 298-355 in: Oxidative Stress and Antioxidant Defenses in Biology.

Ehling-Schulz, M., Schulz, S., Wait, R., Gorg, A. and Scherer S. 2002. The UV-B stimulon of the terrestrial cyanobacterium *Nostoc commune* comprises early shock proteins and late acclimation proteins. Molecular Microbiology 46:827-843.

Folcher, M., Gaillard, H, Nguyen, L.T., Nguyen, K.T., Lacroix, P., Bamas-Jacques, N., Rinkel, M. and Thompson, C.J. 2001. Pleiotropic functions of a *Streptomyces pristinaespiralis* autoregulator receptor in development, antibiotic biosynthesis, and expression of a superoxide dismutase. Journal of Biological Chemistry 276:44297-44306.

Gogorcena, Y., Iturbe-Ormaetxe, I., Escuredo, P.R. and Becana, M. 1995. Antioxidant defenses against activated oxygen in pea nodules subjected to water-stress. Plant Physiology 108:753-759.

Gonzalez-Flecha, B. and Demple, B. 2000. Genetic responses to free radicals. homeostasis and gene control. Annals of the New York Academy of Sciences 899:69-87.

Gunther, C., Schlereth, A., Udvardi, M. and Ott, T. 2007. Metabolism of reactive oxygen species is attenuated in leghemoglobin-deficient nodules of *Lotus japonicus*. Molecular Plant-Microbe Interactions 20: 1596-1603.

Hart, P.J. 2006. Pathogenic superoxide dismutase structure, folding, aggregation and turnover. Current Opinion in Chemical Biology 10:131-138.

Iturbe-Ormaetxe, I. Escuredo, P.R., Arrese-Igor, C. and Becana, M., 1998. Oxidative damage in pea plants exposed to water deficit or paraquat. Plant Physiology 116: 173–181

Kaiser, B.N., Moreau, S., Castelli, J., Thomson, R., Lambert, A., Bogliolo, S., Puppo, A. and Day, D.A. 2003. The soybean NRAMP homologue, GmDMT1, is a symbiotic divalent metal transporter capable of ferrous iron transport. Plant Journal 35:295-304.

Krehenbrink M., and Downie, J.A., 2008. Identification of protein secretion systems and novel secreted proteins in *Rhizobium leguminosarum* bv. viciae. BMC Genomics 9:55-61.

Ken, C.F., Hsiung, T.M., Huang, Z.X., Juang, R.H., and Lin, C.T. 2005. Characterization of Fe/Mn superoxide dismutase from diatom *Thallassiosira weissflogii*: Cloning, expression, and property. Journal of Agricultural and Food Chemistry 53:1470-1474.

Langlois, P., Bourassa, S., Poirier, G.G. and Beaulieu, C. 2003. Identification of *Streptomyces coelicolor* proteins that are differentially expressed in the presence of plant material. Applied and Environmental Microbiology 69:1884-1889.

Li, T., Huang, X., Zhou, R.B., Liu, Y.F., Li, B., Nomura, C., and Zhao, J.D. 2002. Differential expression and localization of Mn and Fe superoxide dismutases in the heterocystous cyanobacterium *Anabaena* sp strain PCC 7120. Journal of Bacteriology 184:5096-5103.

Lobreaux, S., Thoiron, S., and Briat, J.F. 1995. Induction of ferritin synthesis in maize leaves by an iron-mediated oxidative stress. Plant Journal 8:443-449.

McMillan DJ, Davies MR, Good MF, Sriprakash KS (2004) Immune response to superoxide dismutase in group A streptococcal infection. FEMS Immunolgy Medical Microbiology 40:249-256

Madsen, L., Tirichine, L., Jurkiewicz, A., Sullivan, J., Heckmann, A., Bek, A., Ronson, C., James, E.K. and Stougaard, J. 2010. The molecular network governing nodule organogenesis and infection in the model legume *Lotus japonicus*. Nature Communications 1 (DOI: 10.1038/ncomms1009).

Marino, D., Gonzalez, E.M. and Arrese-Igor, C. 2006. Drought effects on carbon and nitrogen metabolism of pea nodules can be mimicked by paraquat: evidence for the occurrence of two regulation pathways under oxidative stresses. Journal of Experimental Botany 57:665-673.

Marino, D., Hohnjec, N., Kuster, H., Moran, J.F., Gonzalez, E.M. and Arrese-Igor, C. 2008. Evidence for transcriptional and post-translational regulation of sucrose synthase in pea nodules by the cellular redox state. Molecular Plant-Microbe Interactions 21:622-630.

Marino, D., Pucciariello, C., Puppo, P. and Frendo, P. 2009 The redox state, a referee of the legume–rhizobia symbiotic game. Advances Botanical Research 52:115-151.

Moran, J.F., James, E.K., Rubio, M.C., Sarath, G., Klucas, R.V. and Becana, M. 2003. Functional characterization and expression of a cytosolic iron-superoxide dismutase from cowpea root nodules. Plant Physiology 133:773-782.

Perry, J.J.P., Shin, D.S., Getzoff, E.D. and Tainer, J.A. 2010. The structural biochemistry of the superoxide dismutases. Biochimica et Biophysica Acta-Proteins and Proteomics 1804:245-262.

Puppo, A., Rigaud, J. and Job, D. 1981. Role of superoxide anion in leghemoglobin autoxidation. Plant Science Letters 22:353-360.

Rubio, M.C., James, E.K., Clemente, M.R., Bucciarelli, B., Fedorova, M., Vance, C. P. and Becana, M. 2004. Localization of superoxide dismutases and hydrogen peroxide in legume root nodules. Molecular Plant-Microbe Interactions 17: 1294-1305.

Rubio, M.C., Becana, M., Kanematsu, S., Ushimaru, T. and James, E.K. 2009. Immunolocalization of antioxidant enzymes in high-pressure frozen root and stem nodules of *Sesbania rostrata*. New Phytologist 183:395-407.

Santos, R., Bocquet, S., Puppo, A. and Touati, D. 1999. Characterization of an atypical superoxide dismutase from *Sinorhizobium meliloti*. Journal of Bacteriology 181:4509-4516.

Santos, R., Herouart, D., Puppo, A. and Touati, D. 2000. Critical protective role of bacterial superoxide dismutase in *Rhizobium*-legume symbiosis. Molecular Microbiology 38:750-759.

Smit W.J., Boquest A.L., Geddes J.E. and Tosolini F.A. 1994. The antibiotic susceptibilities of *Xanthomonas maltophilia* and their relation to clinical management. Pathology. 26:321-324.

Torres, M.A. 2010. ROS in biotic interactions. Physiologia Plantarum 138:414-429.

Trinchant, J. C., Boscari, A., Spennato, G., Van de Sype, G. and Le Rudulier, D. 2004. Proline betaine accumulation and metabolism in alfalfa plants under sodium chloride stress. Exploring its compartmentalization in nodules. Plant Physiology. 135:1583-1594.

Watt, S.A., Wilke, A., Patschkowski, T. and Niehaus, K. 2005. Comprehensive analysis of the extracellular proteins from *Xanthomonas campestris* pv. campestris B100. Proteomics. 5:153-167.

Young, J.P., Crossman, L.C., Johnston, A.W., Thomson, N.R., Ghazoui, Z.F., Hull, K. H., Wexler, M., Curson, A.R., Todd, J.D., Poole, P.S., Mauchline, T.H., East, A.K., Quail, M.A., Churcher, C., Arrowsmith, C., Cherevach, I., Chillingworth, T., Clarke, K., Cronin, A., Davis, P., Fraser, A., Hance, Z., Hauser, H., Jagels, K., Moule, S., Mungall, K., Norbertczak, H., Rabbinowitsch, E., Sanders, M., Simmonds, M., Whitehead, S. and Parkhill, J. (2006) The genome of *Rhizobium leguminosarum* has recognizable core and accessory components. Genome Biol. 7: R34

Zabalza, A., Gálvez, L., Marino, D., Royuela, M., Arrese-Igor, C., and González E.M., 2008. The application of ascorbate or its immediate precursor, galactono-1,4-lactone, does not affect the response of nitrogen-fixing pea nodules to water stress. J. Plant Physiol. 165:805-812

Figure legends

Figure 1. Light microscopy (A, C, E) and transmission electron microscopy (B, D, F) of pea nodules from untreated control plants (A, B), plants treated with 1 µM methylviologen (C, D) and plants treated with 10 µM methylviologen (E, F). (A) Untreated nodules had infected cells (ic) that were healthy in appearance with a regular shape and each had a single central vacuole (*). (B) They contained electron dense bacteroids of *Rhizobium leguminosarum* bv. *viciae*, many of them typically pleiomorphic (b), which were located singly within each symbiosome. Note that there was only a narrow gap between the bacteroids and the symbiosome inner membranes (arrows). n = nucleus. (C) Infected cells in nodules treated with 1 µM methylviologen were less regular in shape and less densely stained than controls, and the vacuoles in many were enlarged (v). Uninfected cells (uc) appeared to be relatively unaffected by the treatment. (D) Bacteroids (b) were less electron dense and many were distorted compared to controls, and the symbiosome spaces (*) were greatly enlarged. (E) Infected cells in nodules treated with 10 µM methylviologen were even more distorted in shape, suggesting a loss of turgor, and very few of them had vacuoles, but many had spaces (*) between the cytoplasm and the cell wall. Uninfected cells (uc) had similar spaces. (F) Bacteroids (b) were still recognizable, but host cell cytoplasm had largely disintegrated with only fragments remaining (arrows). Scale bars, 20 µm (A, C, E), 1 µm (B, D, F).

Figure 2. Inhibitory studies of SOD activity in four week-old pea nodules and leaves. Native gels were pre-incubated either with potassium phosphate buffer (pH 7.8) (A), buffer plus KCN (B) or with buffer plus H_2O_2 (C). All lanes were loaded with 60 µg of protein. Densitometries of the bands from MV-treatment are expressed as percentages relative to the corresponding control bands (lower panel) Values are means ±SE (n=4). NC = control nodules, NMV = methylviologen (MV)-treated nodules, LC = control leaves, LMV = MV-treated leaves.

Figure 3. SOD activity in pea nodules of 3, 4, 6, 8 and 10 week-old *Pisum sativum* cv Snap-pea plants. All lanes were loaded with 45 µg of protein. Densitometry analysis showed no differences between lanes except for nodules on ten week-old plants.

Figure 4. The effect of 24 h of Fe(III) EDTA on the SOD activities in nodule extracts from five week old pea plants. All lanes were loaded with 60 µg of protein. Densitometries of the bands from the Fe-treatment are expressed as percentages relative to the corresponding control bands (lower panel).

Figure 5. SDS-PAGE and Coomassie blue-stained gel showing partial purification of the CamSOD. A similar fraction was run in parallel and the *camSOD* band was transferred to PVDF and used for N-terminal protein sequencing. Molecular weight markers are indicated.

Figure 6. Full length nucleotide sequence of the *sodA* gene from *Rhizobium leguminosarum* and predicted protein sequence (CamSOD). N-terminal residues sequenced by Edman degradation are underlined. The shadowed regions indicate the peptide used for immunization of a rabbit for production of an anti CamSOD antibody.

Figure 7. CamSOD antibody specificity test using as samples pea nodule (N) and non-nodulated plant roots (R). (A) Western-blot with anti-CamSOD after SDS-PAGE. (B) Native gel electrophoresis; two lanes were transferred to a PVDF membrane and used for an immunoblot (left) whilst the other two equivalent lanes were stained for in-gel SOD activity (right).

Figure 8. SDS-PAGE immunoblots of pea nodule extracts (control and MV-treated) with antibodies against either CamSOD (A) or nifDK (B).
1) Free living *Rhizobium leguminosarum* crude extract
2) Pea nodule crude extract
3) Pea nodule bacteroidal fraction
4) Pea nodule plant fraction
5) MV-treated pea nodule crude extract
6) MV-treated pea nodule bacteroidal fraction
7) MV-treated pea nodule plant fraction
8) Pea leaves crude extract.

Figure 9. Immunolocalization of CamSOD in pea nodules. Sections of control nodules are shown in A – D, & F, and a section of a nodule treated with 10 µM Methylviologen is shown in E. (A) Localization of CamSOD on bacteroids (b) and in host cell cytoplasm (arrows). (B) Localization of CamSOD (arrows) on bacteria within an infection thread (it). (C) Localization of CamSOD in the nucleus (n) of an infected cell; note that the chromatin (ch) is also labeled (arrows). (D) Localization of CamSOD on an amyloplast (a) within an uninfected cortical cell (uc) and on mitochondria (arrows) within both infected and uninfected cells. s = starch grain. (E) Localization of CamSOD on bacteroids within a Methylviologen-treated nodule. Note that the bacteroids (b) are distorted in shape and that there only remnants of immunogold labeled cytoplasm (arrows) (cf. Fig. 1F). (F)
Negative control for immunolocalization with pre-immune serum substituted for the CamSOD antibody. Very few gold particles (arrow) are present in any cell compartments, such as bacteroids (b). Bars, 1 µm.

Supplemental Figure Legends

Figure S1. Immunolocalization of the nifH protein of the nitrogenase enzyme complex in pea nodules from untreated control plants (A), plants treated with 1 µM methylviologen (B) and plants treated with 10 µM methylviologen (C). All

sections show labeling exclusively inside the bacteroids (b) (arrows). Bars, 1 µm.

Figure S2. *Rhizobium leguminosarum* CamSOD 3-D model prediction. The sequence of the protein (UniProtKB/TrEMBL Accession number: Q1MJM3-1) was 3-D modeled using the Swiss-Model software of the Swiss Institute of Bioinformatics (http://swissmodel.expasy.org/). The synthetic peptide used for the production of the anti-CamSOD antibody is marked in red.

Figure S3. (A) Probable regulatory elements located up to 400 bp upstream of *SodA* within the *Rhizobium leguminosarum* chromosome. (B) Position of probable promoter boxes upstream from the *SodA* gene that could regulate its expression. Analysis was performed using *Prodic* software.

Figure S4. Mapping of putative coding sequences flanking CamSOD within the *Rhizobium leguminosarum* chromosome. Only sequences that contain a known function or domain are indicated.

Table 1. *Effect of a four day root application of 10 µM methylviologen (MV) on various physiological and biochemical parameters related to growth, photosynthesis, nitrogen fixation and the antioxidant capacity of nodulated pea plants.*

	CONTROL	10 µM MV
Plant DW (g plant^{-1})	0.62 ± 0.08 a	0.51 ± 0.04 b
Photosynthesis (µmol CO_2 m^{-2} s^{-1})*	4.47 ± 0.84 a	2.60 ± 0.37 b
Chlorophylls (SPAD units)*	47.1 ± 2.2 a	37.1 ± 1.6 b
Nitrogen fixation (µmol H_2 g^{-1} NFW min^{-1})*	0.056 ± 0.007 a	0.002 ± 0.001 b
Nodule plant fraction protein (mg g^{-1} NFW)*	10.21 ± 0.71 a	6.63 ± 0.71 b
Nodule bacteroid protein (mg g^{-1} NFW)	5.72 ± 0.40 a	5.11 ± 0.36 a
Leghemoglobin (mg g^{-1} NFW)	0.81 ± 0.20 a	0.14 ± 0.11 b
ASC/DHA	0. 66 ± 0.01 a	0.17 ± 0.02 b
GSH/GSSG	24.2 ± 9.0 a	5.5 ± 0.9 b

*Mean ± SE (n = 6). NFW denotes nodule fresh weight. Numbers followed by a different letter within a row are significantly different at P ≤ 0.05. *Data taken from Marino et al. 2006.*

Figure 1

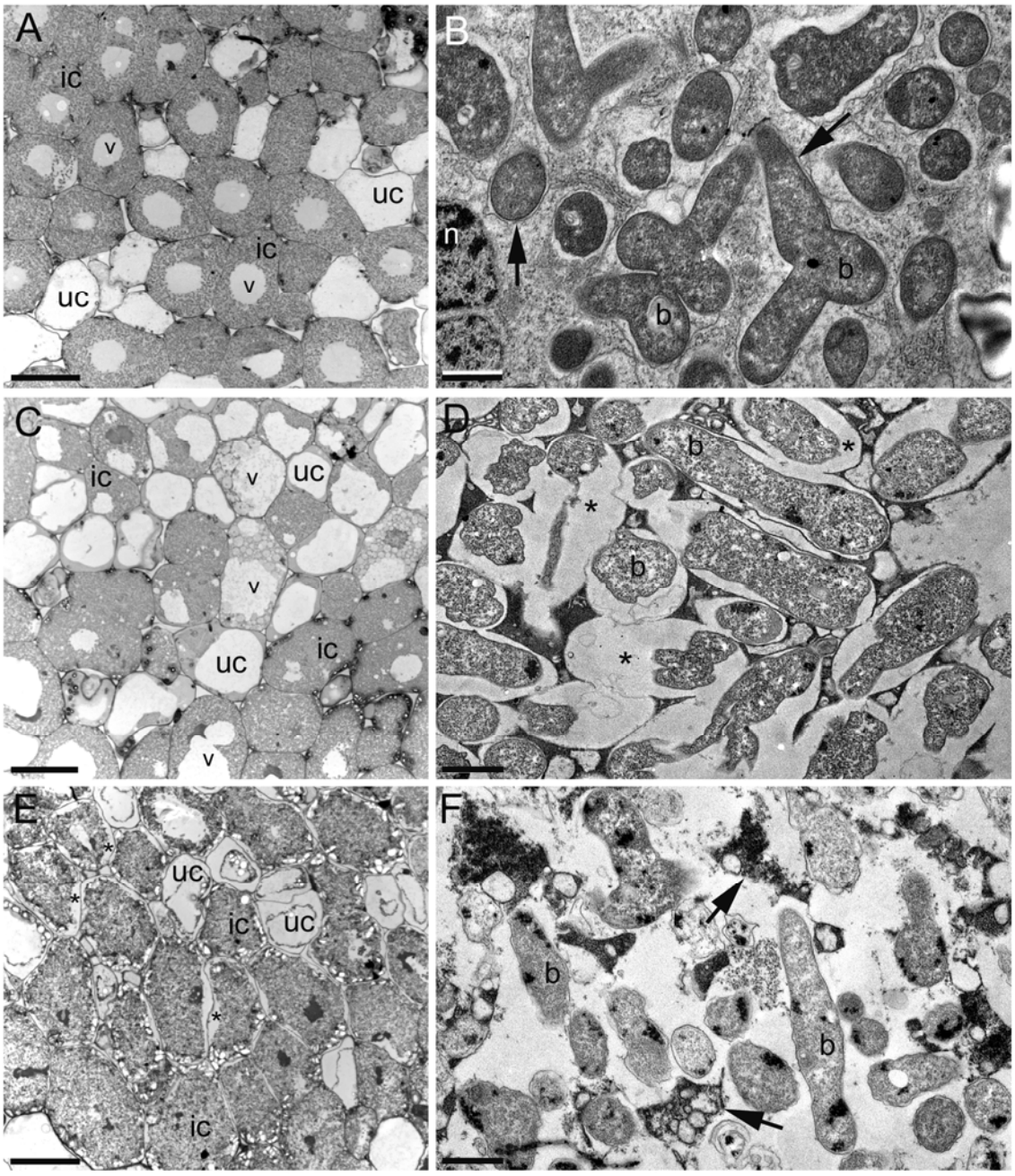

Figure 2

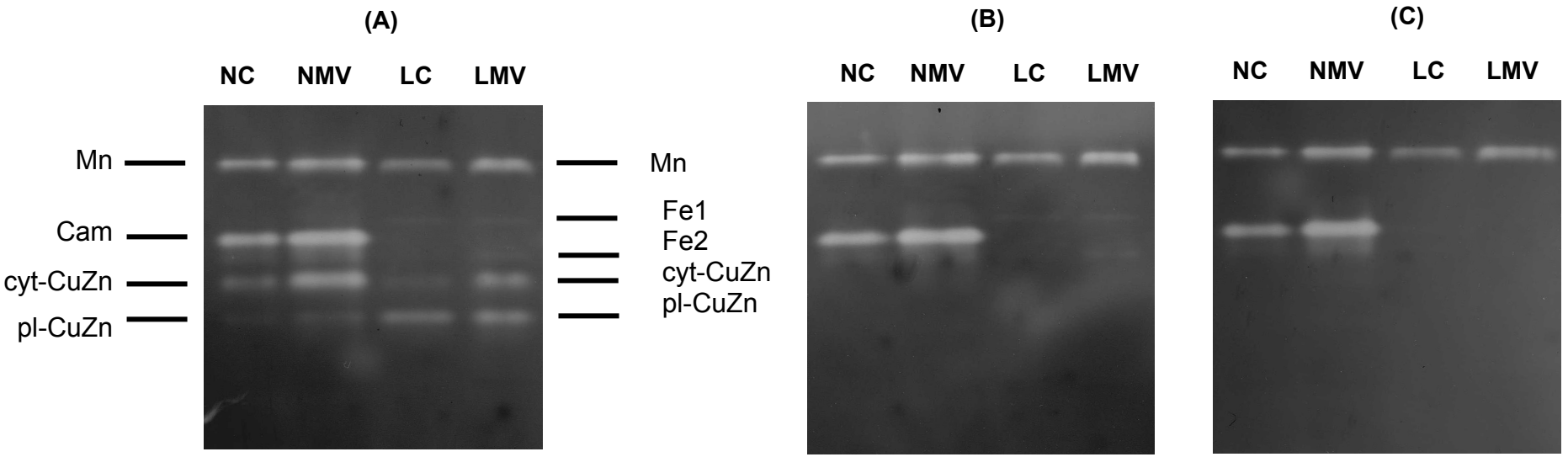

	NC	NMV	LC	LMV
MnSOD	100	130 ± 11	100	125 ± 9
CamSOD	100	184 ± 17	-	-
FeSOD1	-	-	100	99 ± 23
FeSOD2	-	-	100	122 ± 24
Cyt-CuZnSOD	100	257 ± 32	100	212 ± 37
Pl-CuZnSOD	100	170 ± 30	100	114 ± 19

Figure 3

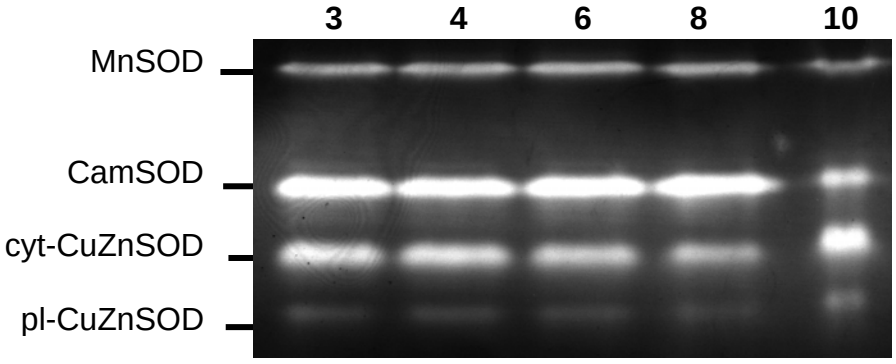

	3	4	6	8	10
MnSOD	100	99	110	112	93
CamSOD	100	92	96	94	75
Cyt-CuZnSOD	100	88	83	78	126
Pl-CuZnSOD	100	95	105	114	186

Figure 4

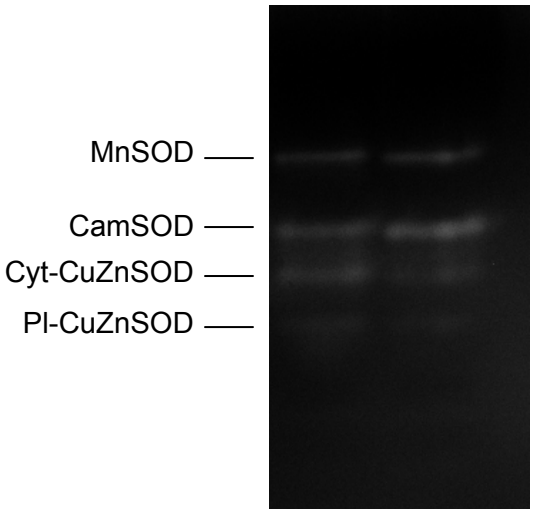

	C	Fe
MnSOD	100	119
CamSOD	100	158
cyt-CuZnSOD	100	50
pl-CuZnSOD	100	56

Figure 5

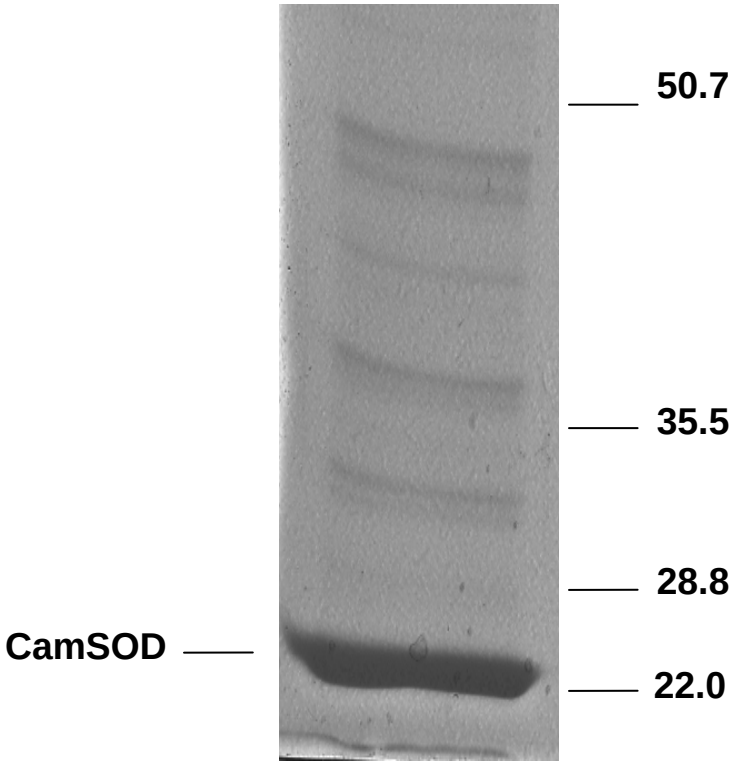

Figure 6

```
atggctttcgaattgcctgaacttccctatgattacgaagcgcttgctcccttcatgtcg  60
  M  A  F  E  L  P  E  L  P  Y  D  Y  E  A  L  A  P  F  M  S  20
aaggaaacgctggagttccaccacgacaagcaccacaaggcctatgtcgacaacggcaac 120
  K  E  T  L  E  F  H  H  D  K  H  H  K  A  Y  V  D  N  G  N  40
aagctcgccgccgaagccggtctttcggacctgtcgctcgaagacgtcgtcaagaagtcc 180
  K  L  A  A  E  A  G  L  S  D  L  S  L  E  D  V  V  K  K  S  60
ttcggcaccaatgccggcctcttcaacaacgcggcccagcactacaaccacatccatttc 240
  F  G  T  N  A  G  L  F  N  N  A  A  Q  H  Y  N  H  I  H  F  80
tggaagtggatgaagaagggcggcggcggcaacaagctgccgggcaagctcgaagcggcc 300
  W  K  W  M  K  K  G  G  G  G  N  K  L  P  G  K  L  E  A  A 100
tttacctccgatctcggcggctacgacaagttcaaggccgatttcgccactgccggcgcc 360
  F  T  S  D  L  G  G  Y  D  K  F  K  A  D  F  A  T  A  G  A 120
acccagttcggctccggctgggcctgggtttccgtcaagaacggcaagctcgaaatctcc 420
  T  Q  F  G  S  G  W  A  W  V  S  V  K  N  G  K  L  E  I  S 140
aagaccccgaacggcgaaaacccgctcgttcacggcgccaccccgatcctcggcgtcgac 480
  K  T  P  N  G  E  N  P  L  V  H  G  A  T  P  I  L  G  V  D 160
gtctgggaacactcctattacatcgactatcgcaacgcccgcccgaaatatctcgaggcc 540
  V  W  E  H  S  Y  Y  I  D  Y  R  N  A  R  P  K  Y  L  E  A 180
ttcgtcgacagcctgatcaactgggactacgtcctggaacgctacgaagcagccacgaag 600
  F  V  D  S  L  I  N  W  D  Y  V  L  E  R  Y  E  A  A  T  K 200
taa
  -
```

Figure 7

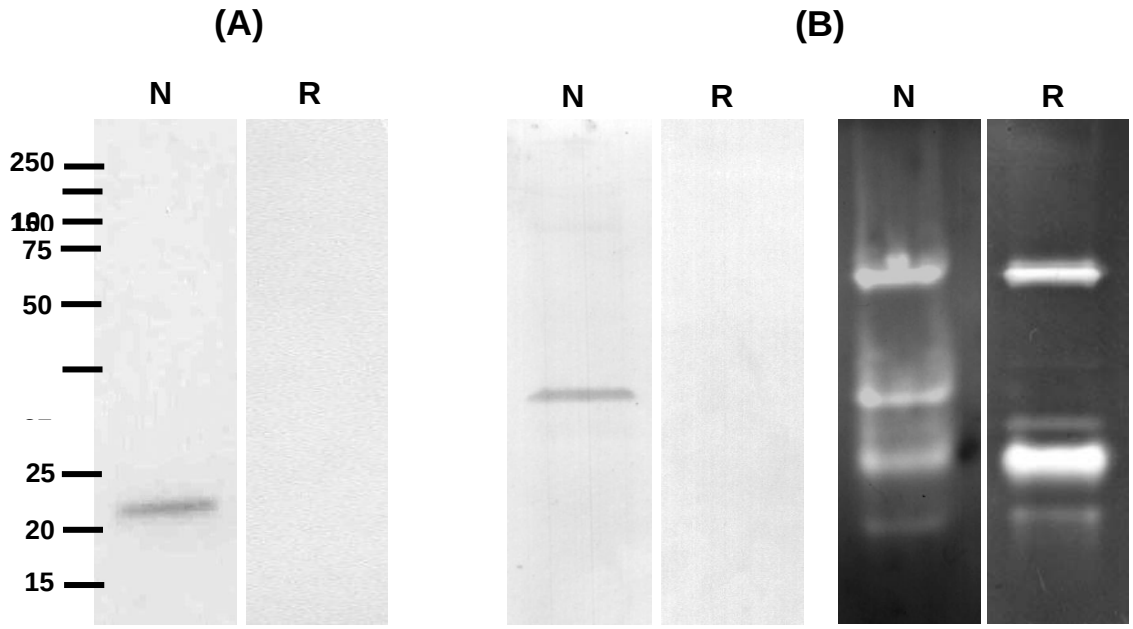

Figure 8

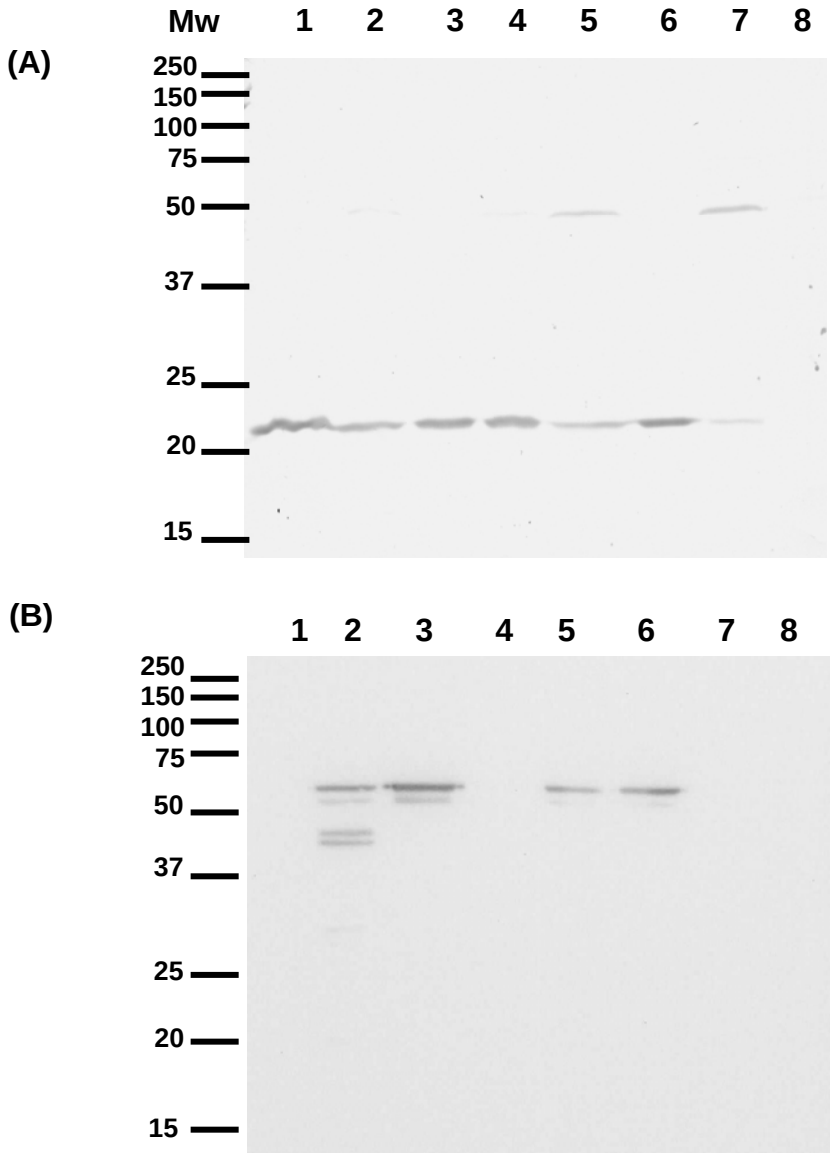
(A)
Mw
1
2
3
4
5
6
7
8
250
150
100
75
50
37
25
20
15
(B)
1
2
3
4
5
6
7
8
250
150
100
75
50
37
25
20
15

Figure 9

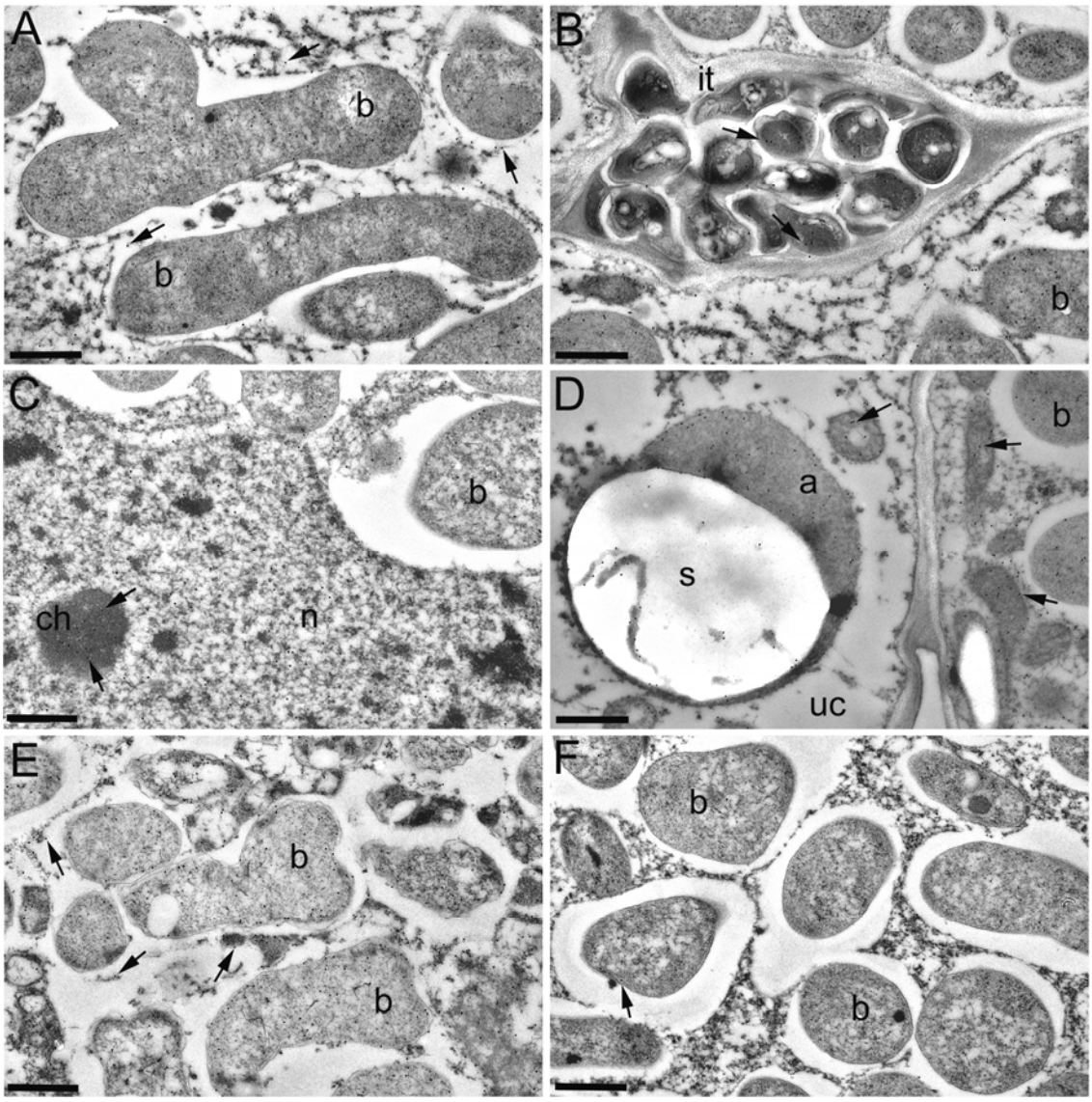

Fig. S1

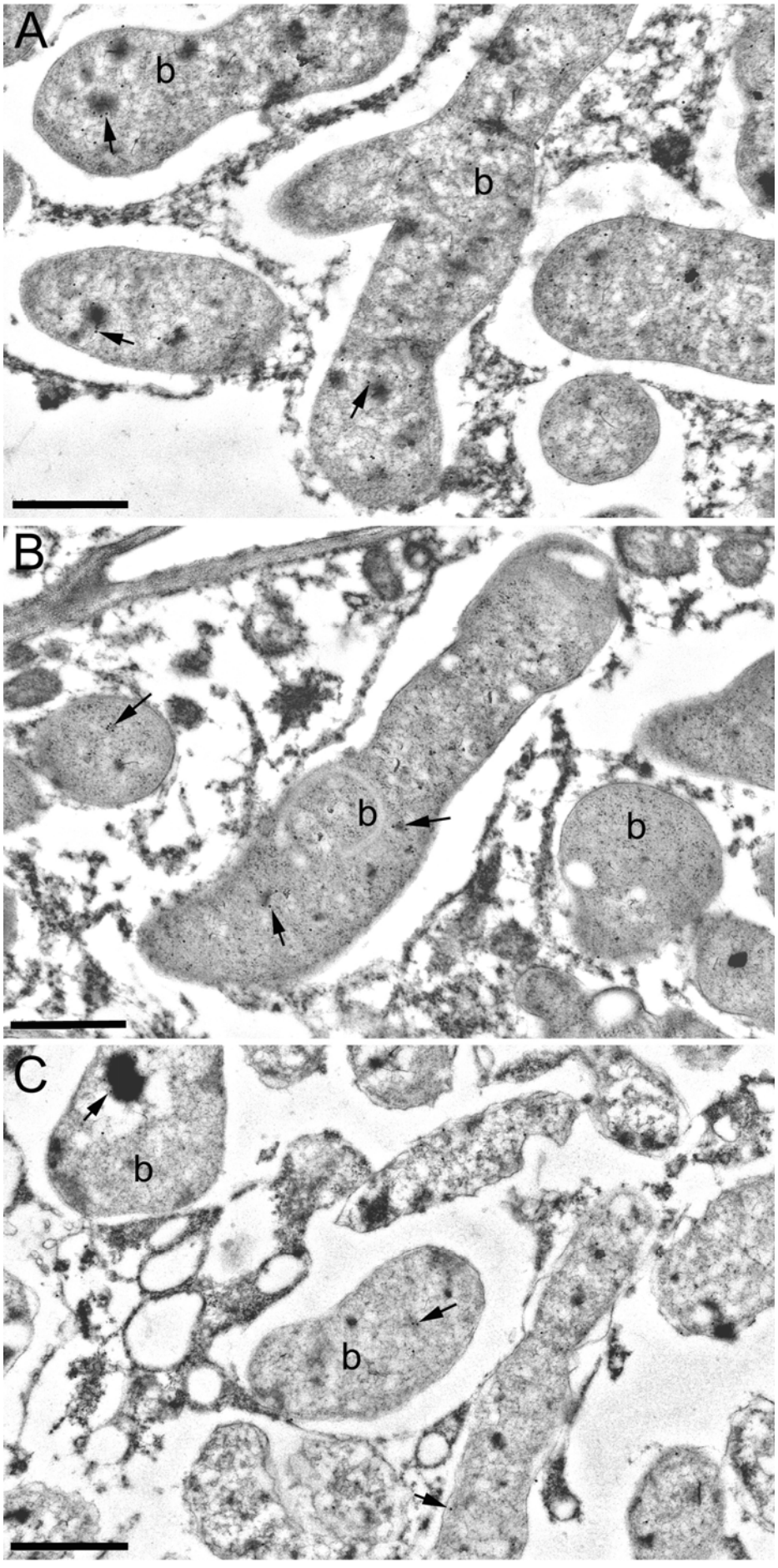

Fig. S2

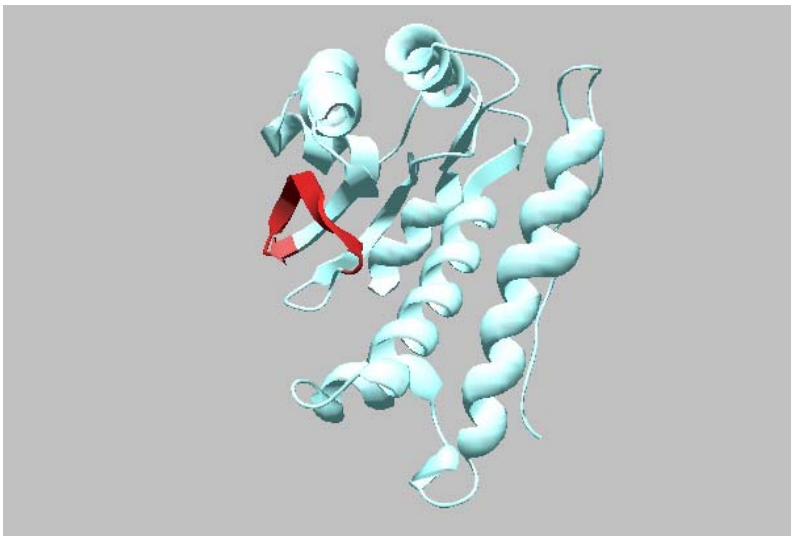

a)

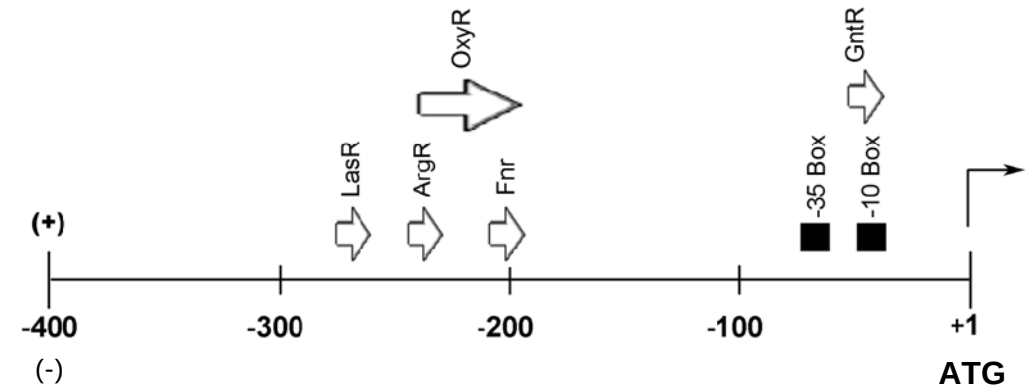

b)

Box	Strand / Position	Score	Organism homology	Promoter function
GntR	(+) 36-51	9.92	*Escherichia coli*	*DNA binding transcriptional repressor*
Fnr	(+) 199-212	8.02	*Escherichia coli*	O_2-regulated via FNR
ArgR	(+) 231-244	9.35	*Escherichia coli*	Arg regulator of the AraC/xylS family and Arg metabolism
OxyR	(+) 196-241	13.78	*Escherichia coli*	Positive regulator of H_2O_2 inducible genes
LasR	(+) 264-279	8.36	*Pseudomonas aeruginosa*	Quorum sensing controlled genes

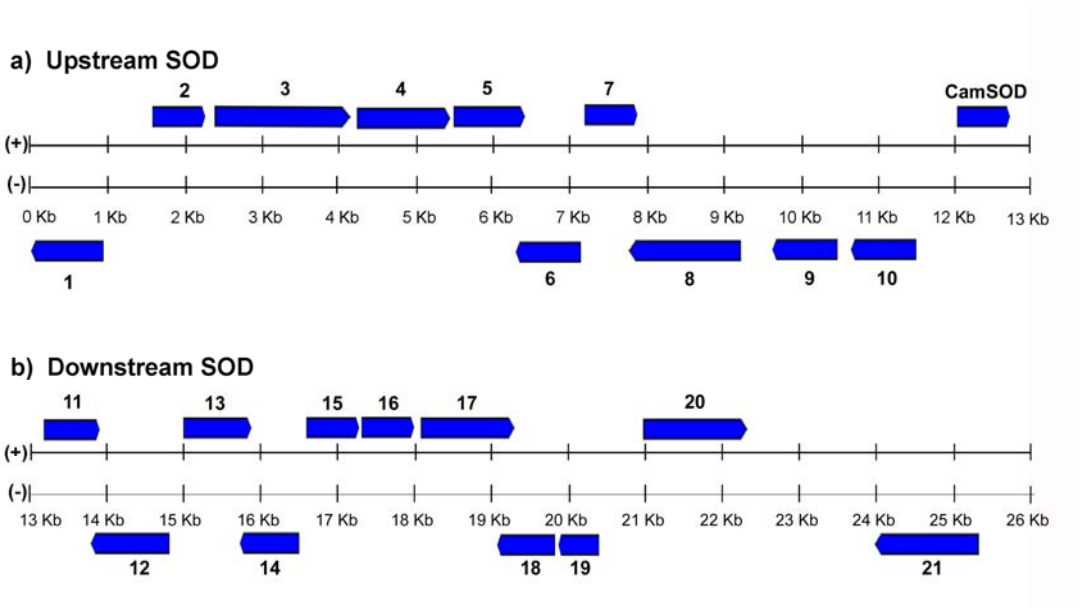

Drug resistance and Xenobiotic detoxification	Metabolic signal and Redox status	Transporters	Regulators
Multidrug resitance efflux pump **(2)**, 420 Aa.	Adenylyl cyclase class 3/4 / Guanylyl cyclase **(4)**, 401 Aa.	Permease protein **(9)**, 243 Aa.	Regulatory protein LysR:LysR, substrate binding **(1)**, 300 Aa.
Drug resistance transporter EmrB/QoCA subfamily **(3)**, 534 Aa.	NAD Synthase **(5)**, 277 Aa.	LysE type translocator, putative aminoacid efflux protein **(15)**, 211 Aa.	Transcriptional regulator, AraC family **(12)**, 302 Aa.
Glutathione S-transferase **(6)**, 227 Aa.	Phosphohydrolases**(11)**, 281 Aa.	Putative acetyl-transferase protein, GNAT family **(19)**, 164 Aa.	Putative transcription regulator protein OR family**(14)**, 230 Aa.
Transcriptional regulatory protein family TetR-N **(7)**, 206 Aa.	Oxide - Reductase **(13)**, 256 Aa.	Histidine-rich transporter transmembrane protein **(20)**, 335 Aa.	
Multidrug resistance efflux pump **(8)**, 512 Aa.	Cytochrome c-556 **(16)**, 146 Aa.		
Phosphatidylethanolamine N-methyltransferase **(10)**, 217 Aa.	Diheme cytochrome c-type signal peptide protein, cytochrome c-553 **(17)**, 304 Aa.		